Nanostructured Polymer Dispersed Liquid Crystals Using a Ferroelectric Smectic a Liquid Crystal

Masaki Yamaguchi , Hiroyuki Matsukizono , Yasushi Okumura , Hirotsugu Kikuchi *

Posted Date: 18 September 2024

doi: 10.20944/preprints202409.1389.v1

Keywords: Polymer dispersed liquid crystals; Memory effect; Birefringence; Molecular orientation

Article

Nanostructured Polymer Dispersed Liquid Crystals Using a Ferroelectric Smectic a Liquid Crystal

Masaki Yamaguchi [1], Hiroyuki Matsukizono [2], Yasushi Okumura [2] and Hirotsugu Kikuchi [2,*]

[1] Interdisciplinary Graduate School of Engineering Sciences, Kyushu University, 6-1 Kasuga-Koen, Kasuga, Fukuoka 816-8580, Japan
[2] Institute for Materials Chemistry and Engineering, Kyushu University, 6-1 Kasuga-Koen, Kasuga, Fukuoka 816-8580, Japan
* Correspondence: kikuchi@cm.kyushu-u.ac.jp; Tel.: +81-92-583-7797

Abstract: Nanostructured polymer dispersed liquid crystals (nano-PDLCs) are transparent and optically isotropic materials, in which submicron-sized liquid crystal (LC) domains are dispersed within a polymer matrix. Nano-PDLCs can induce their birefringence by applying an electric field (*E*-field) based on reorientation of LC molecules. If nano-PDLCs are utilized as light scattering-less birefringence memory materials, it is necessary to suppress the relaxation of LC molecules orientation after removal of the *E*-field. We focused on a ferroelectric smectic A (SmA) to suppress the relaxation of LC molecules due to their layered structure and high viscosity. Although nano-PDLCs require a strong *E*-field to reorient LC molecules due to the anchoring effect on the LC/polymer interface, the required field strength can be reduced by using a ferroelectric smectic A (SmA_F) LC with a large dielectric constant. In this study, we fabricated a nano-PDLC by irradiating an ultraviolet light to a mixture comprising of a SmA_F LC, photocurable monomers and a photo-initiator and its electro-birefringence effect was evaluated using a polarizing optical microscopy. After removal of an *E*-field, enhanced memory effect was observed on the sample using SmA_FLC comparing to nematic LC based nano-PDLCs. (193 words/ **200 words**)

Keywords: polymer dispersed liquid crystals; memory effect; birefringence; molecular orientation

1. Introduction

Polymer-dispersed liquid crystals (PDLCs) are film-like solid composite materials comprising phase-separated liquid crystal (LC) domains and a polymer matrix. Among the multitude of phase separation methods, the most common is polymerization-induced phase separation. This method entails irradiating isotropic solutions of LCs, photocurable monomers, and a photo-initiator with ultraviolet (UV) light. Reorientation of LC molecules by applying an electric field (*E*-field) to PDLCs, which are electro-optical (EO)-responsive materials, has been used in practical applications [1–5]. PDLCs are generally opaque because of their optical inhomogeneity, which causes the transmitted light to scatter. Applying an *E*-field to a PDLC would render it optically uniform and transparent owing to LC reorientation. Additionally, PDLCs exhibit light scattering–light transmission switching upon turning the *E*-field off and on, respectively. This characteristic enables their application as light-regulating materials. Transparent PDLCs (nano-PDLCs), even in the absence of an applied *E*-field, can be obtained by reducing the LC weight fraction in the raw material while increasing the UV irradiation intensity to form a phase-separated structure smaller than the visible wavelength. Nano-PDLCs, such as those with suppressed random light scattering, have been proposed as attractive EO-responsive materials [6–11]. While general PDLCs switch between light scattering and transmission with *E*-field off and on, respectively, nano-PDLCs are initially optically isotropic because of the random orientation of the LC molecules. However, when an *E*-field is applied, the LCs reorient and macroscopic birefringence is induced, exhibiting an electro-birefringence effect. The EO responsivity of nano-PDLCs is also based on the reorientation of LC molecules inside the LC domain by the applied *E*-field. Because of the smaller size of the LC domains, nano-PDLCs require a stronger *E*-field than do general PDLCs for driving because of the large specific surface area of the LC/polymer

 doi:10.20944/preprints202409.1389.v

interface and also the strong influence of interface anchoring. High voltages are required to drive nano-PDLCs. Therefore, attempts have been made to lower the driving voltage by doping nano-PDLCs with conductive materials, [12–14] such as low-T_g polymers [15]. Recently, we realized a transparent PDLC by using a highly polar nematic (N) LC mixture, DIO [16], and its analog compounds. These compounds exhibit large dielectric anisotropy ($\Delta\varepsilon$) values and induce birefringence at low driving voltages. The induced birefringence was partially maintained even after the removal of the *E*-field (memory effect) [17]. In a previous study, the birefringence viewed from the substrate's normal direction was reversibly erased by switching the electrical circuit with a relay switch and applying an *E*-field in the out-of-plane direction of the substrate. Nano-PDLCs exhibit electro-birefringence effect, which is based on the reorientation of LC molecules; the memorized birefringence (up to 50% of induced birefringence) is also derived from the retention of the molecular orientation. The orientation memory effect of LC molecules after the removal of the *E*-field is expected to be more stable in layered structures with mechanical stability and in highly viscous smectic (Sm) LC phases; consequently, Sm LC-based memory-type PDLCs have also been reported [18–20]. In general, the LC molecules in the smectic A (SmA) phase form a layered structure and are more viscous than those in the N phase. Therefore, the threshold voltage required for reorientation by the *E*-field for the SmA phase is higher than that for the N phase. However, the high elastic modulus also suppresses the relaxation of the molecular orientation after the removal of the *E*-field. Therefore, we focused on SmA LCs with high dielectric constants parallel to the LC director. Among the aforementioned DIO analogues, several molecules have been reported to exhibit a ferroelectric SmA (SmA_F) phase with spontaneous polarization parallel to the LC director and dielectric constants reaching several hundred or higher [21,22]. Development of materials that can be driven at voltages lower than the driving voltages of conventional SmA LC-based materials, while exhibiting better retention of molecular orientation than N LCs, can be achieved by using SmA LC materials with greater dielectric anisotropy than that of conventional materials. In this study, we fabricated a transparent PDLC by using a SmA_F LC, EST (previously referred to as EST-4 [22]). The structure and physical properties of the fabricated PDLC were assessed, and the impact of memory effect on the electro-birefringence was investigated.

2. Materials and Methods

2.1. PDLC Sample Preparation

The PDLC precursor was prepared by mixing a 50 wt% (2.73 equiv.) of EST as the SmA_F LC material (synthesized in a prior study [20]); 24.5 wt% (1.0 equiv.) dipentaerythritol hexaacrylate (DPEHA; Tokyo Chemical Industry Co., Ltd.); 24.5 wt% (5.21 equiv.) of *N*-vinyl-2-pyrrolidone (NVP, Tokyo Chemical Industry Co., Ltd.) as photo-polymerizable monomers; and 1 wt% (9.21×10^{-2} equiv.) 2,2-dimethoxy-2-phenylacetophenone (DMPAP, Tokyo Chemical Industry Co., Ltd.) as the photo-initiator. The chemical structures of the PDLC precursors are shown in Figure 5. The hexa-functional acrylic monomer DPEHA was employed for curing in the initial stages of polymerization-induced phase separation. Meanwhile, NVP, a polar vinyl monomer, was also used as a solubilizer for EST, which has a high melting point (100 °C in bulk). The PDLC precursor was injected by utilizing capillary action into an indium tin oxide (ITO)-patterned glass cell (ISSZ-10/B707M7NSS, E. H. C. Co., Ltd.) at 100 °C in an isotropic solution. The UV light (λ = 365 nm peak, 50 mW/cm^2) was then irradiated for 5 min at 110 °C for the photo-polymerization and phase separation to progress, yielding a transparent PDLCs.

 doi:10.20944/preprints202409.1389.v

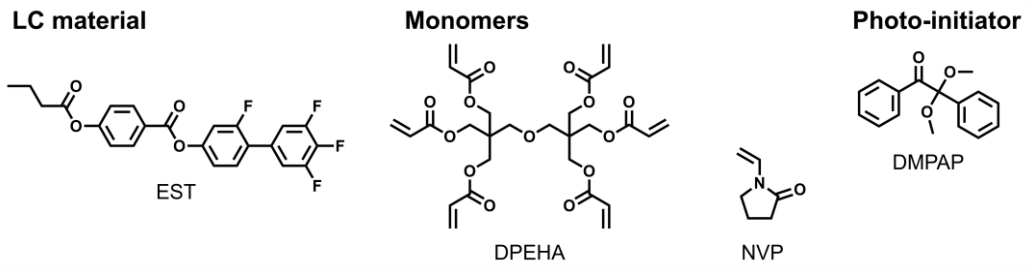

Figure 1. Chemical structure of substances in the PDLC precursor.

2.2. Light Scattering Characterization of PDLC

To investigate the structure of the resulting PDLC, light scattering characterization of the material and the transmitted light intensity was measured using a microscope (Axio Imager.A2M, ZEISS) and a compact instantaneous spectroscopic measurement unit (SA-100S-CK1, LAMBDA VISION Inc.). The normalized transmittance (T) was calculated by measuring the transmitted light intensity in the wavelength range of 400–800 nm and normalizing it by the transmitted light intensity of a toluene-filled cell.

2.3. Scanning Electron Microscopy (SEM) Observation Microscopy Observation of Polymer Matrix

Morphology observation of the polymer matrix was performed using SEM. For SEM observations, the PDLC sample was soaked in dichloromethane to extract the EST molecules and dried thoroughly under vacuum. Finally, the polymer matrix was sputtered with Pt, and the morphology of the polymer matrix was characterized via SEM (Carry Scope JCM5700, JEOL Co., Ltd.) at an accelerating voltage of 5 kV.

2.4. Differential Scanning Calorimetry (DSC) Measurements

Differential scanning calorimetry (DSC) measurements of the PDLC sample was performed to investigate the phase transition behavior of EST in a fine polymer matrix. DSC curves were recorded using a differential scanning calorimeter (DSC 1 STAR^e System, Mettler Toledo, Switzerland) with a dedicated aluminum pan, at a scanning rate of 5 °C/min.

2.5. Dielectric Spectroscopy of PDLC

The dielectric relaxation spectra of the PDLC were recorded in the range of 1 Hz to 1 1 MHz using an impedance/gain phase analyzer (SI 1260, Solartron Metrology) at an applied voltage of 0.1 V. Cells were used with no surface orientation treatment, an ITO electrode area of 1 cm^2, and a cell thickness of 10 μm (KSSZ-10/B107M6NSS05, E.H.C Co., Ltd). First, the ITO electrode resistance and capacitance were measured using an empty cell, which was used to correct the PDLC impedance and obtain the PDLC dielectric constants. After measuring the empty-cell resistance and capacitance, the precursor was injected into the cell and photo-polymerized under UV irradiation.

2.6. Electro-Birefringence Effect

The electro-birefringence effect of the PDLC samples was measured using a polarizing optical microscope (ECLIPSE LV100 POL, Nikon), with a DS-Ri1 camera, under crossed polarizers and by applying a sine-wave *E*-field parallel to the substrate plane with frequency ranging from 10 Hz to 10 kHz. To determine the frequency characteristics of the electro-birefringence effect of the PDLC sample, the optical retardation (at 536 nm) of each PDLC sample was measured using Berek compensator (Nichika Co., Ltd.). The birefringence (Δn) was calculated by dividing the optical retardation by the cell thickness (10 μm).

3. Results and Discussion

At temperatures over 80 °C, where EST exhibits LC phases, the PDLC exhibited higher normalized transmittance ($T > 0.7$), suggesting the formation of phase-separated structures smaller

 doi:10.20944/preprints202409.1389.v

than visible light wavelength (Figure 2). Furthermore, T was found to decrease with decreasing temperature. This decrease in T can be attributed to the slight coarsening of the phase-separated LC domains due to the lowering of the compatibility between the EST molecules and polymer matrix with decreasing temperature. The SEM images show a phase separation of approximately 60–120 nm in size with a polymer ball-type morphology (Figure 2 inset and Figure S1 in the Supporting Information). LC droplet structures have not been observed in the memory PDLCs with micrometer-sized phase-separated structures [23]. However, a similar polymer morphology was observed in this study.

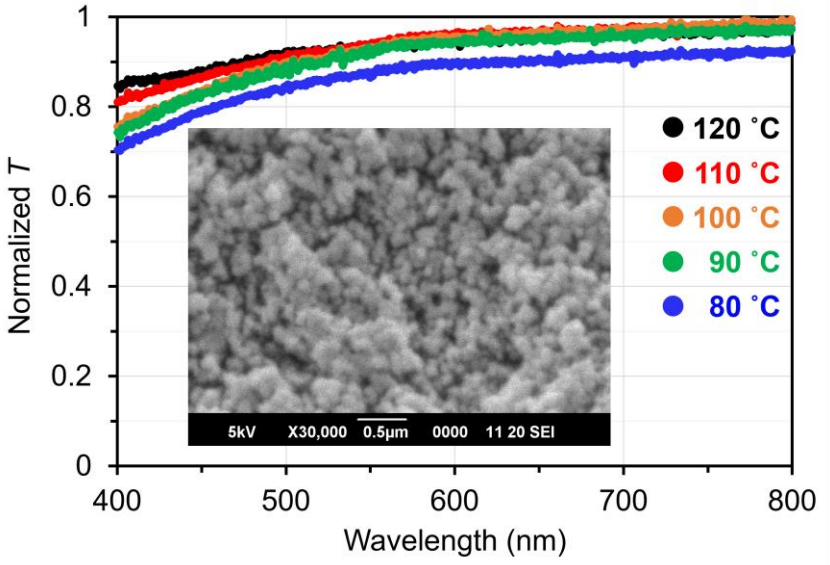

Figure 2. Transmittance of the PDLC normalized with a toluene-filled cell. Inset: SEM image of PDLC of polymer matrix.

All the observed phase transition points, both during heating and cooling, shifted toward lower temperatures than those of the bulk EST [22]. In the cooling step, exothermic peaks were observed at 130 °C (Iso. to N), 111 °C (N to SmA_F), and 74 °C (SmA_F to Cr.), depending on phase transition (Figure 3A). Furthermore, the phase transition enthalpy of EST in the PDLC were clearly lower than that of the bulk—0.328 kJ/mol, 1.18 kJ/mol, and 15.1 kJ/mol, which were 78%, 45%, and 56% of that of the bulk, respectively. The small apparent enthalpies of phase transition observed in the DSC measurements is attributable to the fact that many of the ESTs dissolved in the polymer matrix or were dispersed to such a small size that they did not exhibit phase transition. The lower transition point of the Iso. to N in the PDLC as compared to the bulk LC suggests a higher solubility or affinity between the LC and polymer [24]. Furthermore, the broadening of each phase transition peak in the DSC curves suggests that materials undergoing phase transitions are thermally destabilized and that their degree of destabilization varies widely. The phase transitions of EST proceed over a broad temperature range, indicating that EST molecules adopt various states in the polymer matrix.

 doi:10.20944/preprints202409.1389.v

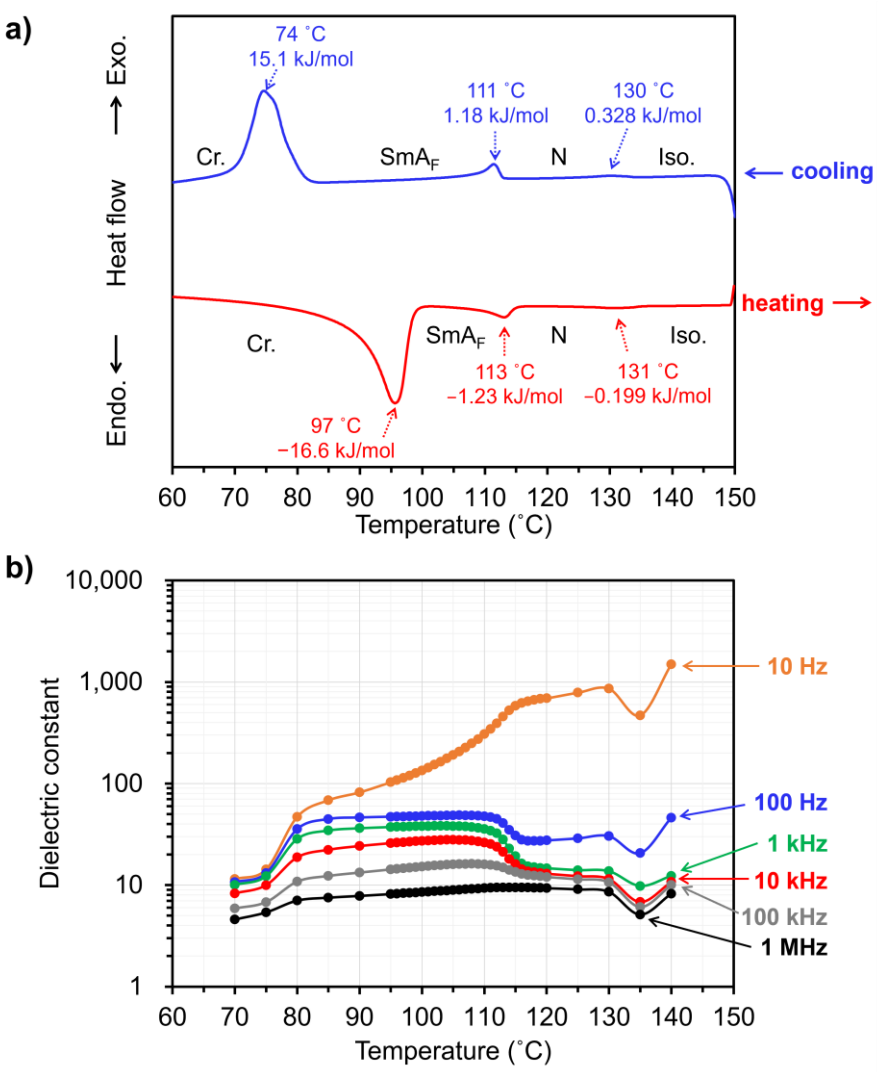

Figure 3. (a) DSC curves of the PDLC; scanning rate: 5 °C/min. (b) Temperature dependence of the dielectric constant (ε') of the PDLC at various frequencies.

Next, dielectric measurements were performed to investigate the relationship between the phase transitions and electrical properties of the PDLC. The dielectric constants (ε') of the PDLC was measured within the range of 130–70 °C during the cooling process, as shown in Figure 3B. A comparison of the temperature dependence of ε' at different frequencies indicates that the magnitude of ε' tends to be smaller at higher frequencies, with a large change in ε' between 115 and 110 °C at all frequencies. This marked temperature-dependent change in ε' may be associated with the change in *E*-field responsivity due to the SmA_F to N phase transition of the dispersed EST molecules in the polymer matrix. The ε' value is large in the low-frequency range; however, the large apparent ε' may include the conductive components of small amounts of adsorbed water in the material and small amounts of ionic conductive impurities. In addition, the LC domains in insulating polymer matrix is less likely to be subjected to the E-field, which should be considered in the low-frequency range [25]. As evident from the DSC curves in Figure 3A, the change in electrical properties around 115–110 °C can be attributed to the phase transition of EST molecules.

As regards Δn values, $\Delta n_{app.}$ and $\Delta n_{rem.}$ denote the Δn values during the application of an *E*-field and that after the removal of an *E*-field, respectively. As shown in Figures 4A, 4D and 4G, before the application of the *E*-field, the PDLC sample does not show Δn and does not transmit light in the polarizing optical microscopy (POM) observation under crossed nicols. When a voltage of 100 V was applied at a frequency of 10 kHz, $\Delta n_{app.}$ was induced by the *E*-field because light was transmitted between the electrodes (Figures 4B, 4E, and 4H). The same procedure was also used to measure $\Delta n_{app.}$

 doi:10.20944/preprints202409.1389.v

at frequencies of 1 kHz, 100 Hz, and 10 Hz, at various temperatures, when 100 V was applied. A comparison of $\Delta n_{app.}$ during the application of 100 V at various frequencies indicates that larger $\Delta n_{app.}$ values were observed at higher frequencies. This is contrary to the trend of ε', wherein larger ε' values were observed at lower frequencies. This result suggests that when 100 V is applied to the PDLC, a sufficient voltage is not applied to the EST-rich domain to reorient the EST molecules unless it is in the high-frequency range of approximately 1 kHz or higher. If larger phase-separated structures were obtained, the PDLC would exhibit higher light scattering; however, a larger $\Delta n_{app.}$ would be induced. $\Delta n_{app.}$ was almost zero during the application of 100 V in the case of a transparent PDLC with an SmA LC, 4-cyano-4′-*n*-octyloxybiphenyl (8OCB). This also confirms that this PDLC using EST is more EO-responsive compared to other SmA LC-based materials. After the removal of the *E*-field, $\Delta n_{rem.}$ decreased significantly as only a small amount of light is transmitted between the electrodes at 115 °C (Figure 4C). Meanwhile, at 110 and 100 ˚C, the light intensity transmitted between the electrodes was higher (brighter), indicating the retention of larger Δn_{rem} values (Figures 4F and 4I). The retention of $\Delta n_{rem.}$ after the removal of the *E*-field indicates that the EST molecules did not completely relax to their initial (random) molecular orientation after the removal of the *E*-field and that the molecular orientation induced by the *E*-field was partially maintained. $\Delta n_{rem.}$ was completely erased upon heating the sample above 130 ˚C.

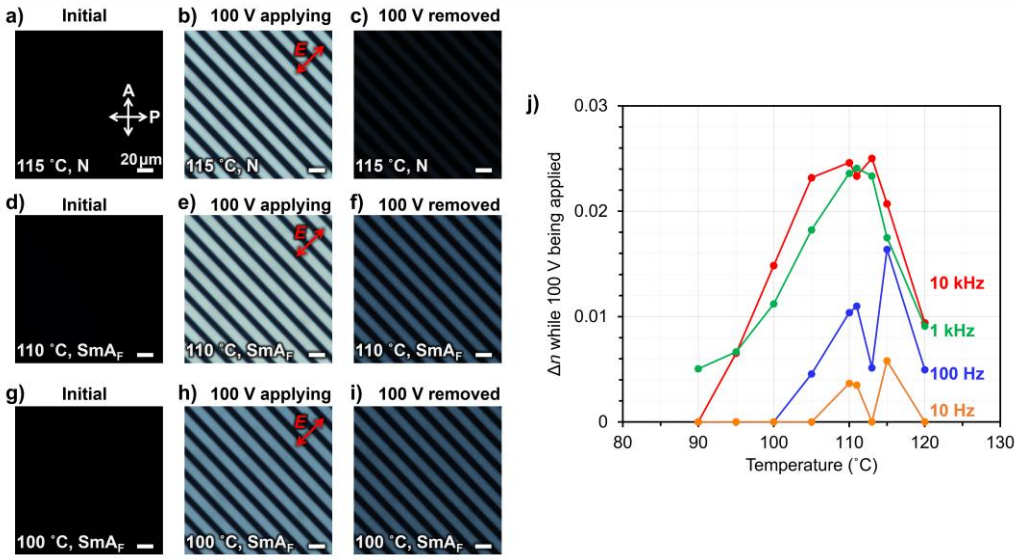

Figure 4. (a), (d), (g) POM images of the PDLC before applying an *E*-field at 115, 110, and 100 °C. (b), (e), (h) POM images of PDLC during application of 100 V with a frequency of 10 kHz at 115, 110, and 100 °C. (c), (f), (i) POM images of the PDLC after removing the *E*-field at 115, 110, and 100 °C. (j) Temperature dependence of *E*-field induced Δ*n* during application of 100 V at various frequencies.

The relationship between the Δ*n* memory properties and temperatures after the removal of the *E*-field was meticulously investigated for the frequencies of 1 kHz and 10 kHz, where the better electro-birefringence effects were observed. The proportion of Δ*n* memorized after the removal of the *E*-field was defined as the memory retention rate, MRR, which is calculated as follows:

$$\mathrm{MRR}\ /\ \% \equiv \frac{\Delta n_{rem.}}{\Delta n_{app.}} \times 100. \qquad (1)$$

As regards the temperature dependence of MRR, it is less than 40% above 111 °C, indicating that EST is considered to be the N phase in the PDLC sample. However, below 100 °C, where the EST is considered to have completely transitioned to SmA$_F$, the MRR is more than 60%. These features were similar at the frequencies of 1 and 10 kHz (Figure 5). As evident from the DSC curve in Figure 3A, the phase transition from N to SmA$_F$ proceeds within broad temperature ranges; the MRR was not likely to be high given the presence of both SmA$_F$ phase and N phase at 110 °C. At higher temperatures, the MRR is less than 40% because of the relaxation of the molecular orientation of the EST to the initial orientation upon the removal of the *E*-field. In contrast, in the temperature range of

 doi:10.20944/preprints202409.1389.v

the SmA_F phase, the elastic modulus of EST was relatively higher than that of the N phase, and the relaxation of the molecular orientation after the removal of the *E*-field was apparently suppressed. In addition, when a triangular-waveform *E*-field was applied to the material, currents due to polarization reversal were observed, confirming its ferroelectricity (Figure S2 in the Supporting Information).

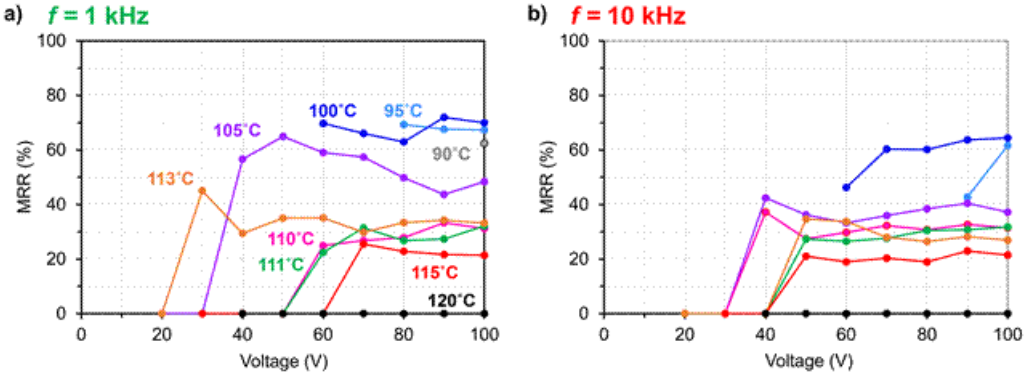

Figure 5. MRR in the temperature range 120-90 °C at the frequency of (a)1 kHz and (b) 10 kHz.

Previously, we fabricated N LC-based nano-PDLCs with phase-separated structure sizes of 100–200 nm, with an MRR of at most 50% [17]. The material in this study used the polar monofunctional vinyl monomer NVP, which was thought to provide a polar anchoring force between the polymer interface and the EST molecules. The anchoring effect was expected to be stronger in the nano-PDLC in this study than in the previous study because of the lower LC constitutive fraction and smaller phase-separated structure; further, the previous work did not use NVP as the monomer. Because anchoring at the interface with the polymer is the driving source of LC reorientation after the removal of the *E*-field, a strong anchoring effect is disadvantageous for the memory effect. The high MRR (70%) in this study, despite stronger anchoring than in previous studies, indicates that the ability of SmA_F LC to retain molecular orientation after *E*-field removal is beneficial. Because the LC domains within the nano-PDLCs are remarkably fine, the LC confined within them are subjected to large deformations. In the memory state of nano-PDLCs, slight deformations of the Sm layers and presence of minor defects may be acceptable; conversely, large layer deformations and presence of numerous defects would lead to memory degradation [20]. The loss of approximately 30% of the Δn memory is apparently due to the complex polymer structure and anchoring forces that distort the molecular orientation of EST near the polymer interface. This results in the inability to maintain a Sm layered structure near the polymer, as well as a partial N-like orientation ordering and enhanced relaxation. The anchoring of polymers with large polarities may be effective in maintaining the molecular orientation by retaining the ferroelectric polarization of EST molecules. This PDLC fabricated in this study can be driven at voltages lower than the driving voltages of conventional SmA LC-based materials. It can also be pinned at any Δn value more efficiently than N LC-based materials, making it suitable for applications such as display elements without viewing angle dependence and electrically tunable micro lenses.

4. Conclusions

A PDLC exhibiting high transparency in the visible wavelength range was fabricated using SmA_F LC, photopolymerizable monomers, and a photo-initiator. SEM observations revealed the formation of a fine polymer-ball morphology with a size of 60–120 nm; no LC droplet morphology was observed. The phase transition behavior of the LC molecules in the PDLC was investigated using DSC; the results suggest strong interactions between the polymer matrix and LC molecules. Fu.rthermore, with regard to the electro-birefringence effect, different electric birefringence responses were observed, depending on the phase transition of the LCs in the PDLC. After the LCs transition from the N phase to the SmA_F phase, the proportion of memorized Δn retained after the removal of

the *E*-field increased, suggesting enhanced molecular orientation memory based on mechanical stability in the SmA_F phase. They can be driven at voltages lower than the driving voltages of conventional materials using SmA LC. In addition, the molecular orientation memory, which was enhanced in the SmA_F phase, was stable after the removal of the *E*-field. These PDLCs will potentially aid the development of applications such as display elements without view-angle dependence and electrically tunable microlenses.

Supplementary Materials: The following supporting information can be downloaded at: www.mdpi.com/xxx/s1, Figure S1: SEM images of polymer matrix at different magnifications.; Figure S2: a) Switching current response of the PDLC while applying a triangular-wave *E*-field. B) Hysteresis between the electric flux density and voltage measured in SmA_F phase.

Author Contributions: Conceptualization, H.K.; methodology, H.K.; software, Y.O.; validation, M.Y.; formal analysis, M.Y.; investigation, M.Y.; resources, H.K., Y.O. and H.K.; data curation, M.Y.; writing—original draft preparation, M.Y.; writing—review and editing, H.M., Y.O. and H.K.; visualization, M.Y.; supervision, H.K.; project administration, H.K.; funding acquisition, H.K. All authors have read and agreed to the published version of the manuscript.

Funding: This research was funded by JSPS KAKENHI, Grant Numbers JP23H00303 and JP23K17366. MEXT Project "Integrated Research Consortium on Chemical Sciences (IRCCS)," Dynamic Alliance for Open Innovation Bridging Human, Environment and Materials from the Ministry of Education, Culture, Sports, Science and Technology, Japan (MEXT), and the Cooperative Research Program of "Network Joint Research Center for Materials and Device.".

Institutional Review Board Statement: Not applicable.

Informed Consent Statement: Not applicable.

Data Availability Statement: Data are contained within the article.

Acknowledgments: The authors would like to thank Editage (www.editage.jp) for English language editing.

Conflicts of Interest: The authors declare no conflicts of interest.

References

1. Kajiyama, T.; Miyamoto, A.; Kikuchi, H.; Morimura, Y. AGGREGATION STATES AND ELECTRO-OPTICAL PROPERTIES BASED ON LIGHT-SCATTERING OF POLYMER (LIQUID-CRYSTAL) COMPOSITE FILMS. *Chemistry Letters* **1989**, 813-816, doi:10.1246/cl.1989.813.
2. KAJIYAMA, T.; KIKUCHI, H.; MIYAMOTO, A.; MORITOMI, S.; HWANG, J. AGGREGATION STATES AND BISTABLE LIGHT SWITCHING OF (LIQUID-CRYSTALLINE POLYMER) (LOW-MOLECULAR WEIGHT LIQUID-CRYSTAL) MIXTURE SYSTEMS. *CHEMISTRY LETTERS* **1989**, 817-820.
3. Doane, J.W.; Golemme, A.; West, J.L.; Whitehead, J.B.; Wu, B.G. POLYMER DISPERSED LIQUID-CRYSTALS FOR DISPLAY APPLICATION. *Molecular Crystals and Liquid Crystals* **1988**, *165*, 511-532, doi:10.1080/00268948808082211.
4. Zumer, S.; Doane, J.W. LIGHT-SCATTERING FROM A SMALL NEMATIC DROPLET. *Physical Review A* **1986**, *34*, 3373-3386, doi:10.1103/PhysRevA.34.3373.
5. Wu, B.G.; Erdmann, J.H.; Doane, J.W. RESPONSE-TIMES AND VOLTAGES FOR PDLC LIGHT SHUTTERS. *Liquid Crystals* **1989**, *5*, 1453-1465, doi:10.1080/02678298908027783.
6. Bunning, T.J.; Natarajan, L.V.; Tondiglia, V.P.; Sutherland, R.L. Holographic polymer-dispersed liquid crystals (H-PDLCs). *Annual Review of Materials Science* **2000**, *30*, 83-115, doi:10.1146/annurev.matsci.30.1.83.
7. Aya, S.; Le, K.V.; Araoka, F.; Ishikawa, K.; Takezoe, H. Nanosize-Induced Optically Isotropic Nematic Phase. *Japanese Journal of Applied Physics* **2011**, *50*, doi:10.1143/jjap.50.051703.
8. Verbrugge, V.; de la Tocnaye, J.; Dupont, L. C-band wavelength-tunable vertical-cavity laser using a nano polymer dispersed liquid crystal material. *Optics Communications* **2003**, *215*, 353-359, doi:10.1016/s0030-4018(02)02118-1.
9. Levallois, C.; Verbrugge, V.; Dupont, L.; de la Tocnaye, J.L.B.; Caillaud, B.; Le Correa, A.; Dehaese, O.; Folliot, H.; Loualiche, S. 1.55-mu m optically pumped tunable VCSEL based on a nano-polymer dispersive liquid crystal phase modulator. In Proceedings of the Conference on Micro-Optics, VCSELs, and Photonic Interconnects II, Strasbourg, FRANCE, Apr 03-05, 2006.

10. Matsumoto, S.; Houlbert, M.; Hayashi, T.; Kubodera, K. Fine droplets of liquid crystals in a transparent polymer and their response to an electric field. *Applied Physics Letters* **1996**, *69*, 1044-1046, doi:10.1063/1.116925.
11. Pagidi, S.; Manda, R.; Bhattacharyya, S.S.; Lee, S.G.; Song, S.M.; Lim, Y.J.; Lee, J.H.; Lee, S.H. Fast Switchable Micro-Lenticular Lens Arrays Using Highly Transparent Nano-Polymer Dispersed Liquid Crystals. *Advanced Materials Interfaces* **2019**, *6*, doi:10.1002/admi.201900841.
12. Pagidi, S.; Srivastava, A.; Pandey, N.; Manda, R. Reduced driving electric field of ionic salt doped nano-structured polymer dispersed liquid crystals device. *JOURNAL OF MOLECULAR LIQUIDS* **2024**, *399*, doi:10.1016/j.molliq.2024.124444.
13. Pagidi, S.; Manda, R.; Bhattacharyya, S.S.; Cho, K.J.; Kim, T.H.; Lim, Y.J.; Lee, S.H. Superior electro-optics of nano-phase encapsulated liquid crystals utilizing functionalized carbon nanotubes. *Composites Part B-Engineering* **2019**, *164*, 675-682, doi:10.1016/j.compositesb.2019.01.091.
14. Pagidi, S.; Manda, R.; Shin, H.S.; Lee, J.; Lim, Y.J.; Kim, M.; Lee, S.H. Enhanced electro-optic characteristics of polymer-dispersed nano-sized liquid crystal droplets utilizing PEDOT:PSS polymer composite. *Journal of Molecular Liquids* **2021**, *322*, doi:10.1016/j.molliq.2020.114959.
15. Pagidi, S.; Park, H.; Lee, D.; Kim, M.; Lee, S.H. Nanosize-confined nematic liquid crystals at slippery interfaces of polymer composites consisting of poly (hexyl methacrylate). *Journal of Molecular Liquids* **2022**, *350*, doi:10.1016/j.molliq.2022.118540.
16. Nishikawa, H.; Shiroshita, K.; Higuchi, H.; Okumura, Y.; Haseba, Y.; Yamamoto, S.I.; Sago, K.; Kikuchi, H. A Fluid Liquid-Crystal Material with Highly Polar Order. *Advanced Materials* **2017**, *29*, doi:10.1002/adma.201702354.
17. Yamaguchi, M.; Okumura, Y.; Nishikawa, H.; Matsukizono, H.; Kikuchi, H. Memorizable Electro-Birefringence Effect Exhibited by Transparent Liquid Crystal/Polymer Composite Materials. *ADVANCED ELECTRONIC MATERIALS* **2024**, doi:10.1002/aelm.202400055.
18. Kikuchi, H.; Moritomi, S.; Hwang, J.; Kajiyama, T. Bistable Electro-optical Switching for (Liquid Crystalline Polymer)/(Low Molecular Weight Liquid Crystal) Composite System. *POLYMERS FOR ADVANCED TECHNOLOGIES* **1990**, *1*, 297-303.
19. FUH, A.; KO, T.; LI, M. POLYMER DISPERSED LIQUID-CRYSTAL FILMS WITH MEMORY CHARACTERISTICS. *JAPANESE JOURNAL OF APPLIED PHYSICS PART 1-REGULAR PAPERS SHORT NOTES & REVIEW PAPERS* **1992**, *31*, 3366-3369.
20. Date, M.; Takeuchi, Y.; Kato, K. Droplet size effect on the memory-mode operating temperature of smectic-A holographic polymer dispersed liquid crystal. *JOURNAL OF PHYSICS D-APPLIED PHYSICS* **1999**, *32*, 3164-3168.
21. Kikuchi, H.; Matsukizono, H.; Iwamatsu, K.; Endo, S.; Anan, S.; Okumura, Y. Fluid Layered Ferroelectrics with Global $C_{\infty v}$ Symmetry. *ADVANCED SCIENCE* **2022**, *9*, doi:10.1002/advs.202202048.
22. Matsukizono, H.; Sakamoto, Y.; Okumura, Y.; Kikuchi, H. Exploring the Impact of Linkage Structure in Ferroelectric Nematic and Smectic Liquid Crystals. *JOURNAL OF PHYSICAL CHEMISTRY LETTERS* **2024**, *15*, 4212-4217, doi:10.1021/acs.jpclett.3c03492.
23. Yamaguchi, R.; Sato, S. MEMORY EFFECTS OF LIGHT TRANSMISSION PROPERTIES IN POLYMER-DISPERSED-LIQUID-CRYSTAL (PDLC) FILMS. *Japanese Journal of Applied Physics Part 2-Letters* **1991**, *30*, L616-L618, doi:10.1143/jjap.30.l616.
24. Mucha, M. Polymer as an important component of blends and composites with liquid crystals. *PROGRESS IN POLYMER SCIENCE* **2003**, *28*, 837-873.
25. Miyamoto, A.; Kikuchi, H.; Kobayashi, S.; Morimura, Y.; Kajiyama, T. DIELECTRIC PROPERTY ELECTROOPTICAL EFFECT RELATIONSHIPS OF POLYMER LIQUID-CRYSTAL COMPOSITE FILMS. *Macromolecules* **1991**, *24*, 3915-3920, doi:10.1021/ma00013a027.